Measurement 87 (2016) 274–293

Contents lists available at ScienceDirect

Measurement

journal homepage: www.elsevier.com/locate/measurement

A quadratic polynomial signal model and fuzzy adaptive filter for frequency and parameter estimation of nonstationary power signals

Sarita Nanda [a], P.K. Dash [b,*], Tatiana Chakravorti [b], Shazia Hasan [c]

[a] KIIT University, Bhubaneswar, India
[b] Siksha O Anusandhan University, Bhubaneswar, India
[c] BITS, Dubai, United Arab Emirates

ARTICLE INFO

Article history:
Received 24 April 2015
Received in revised form 10 January 2016
Accepted 12 March 2016
Available online 17 March 2016

Keywords:
ADALINE
Fuzzy logic based step size
Gauss–Newton method
Frequency deviation
Phasor estimation
Power system transient

ABSTRACT

Accurate estimation of amplitude, phase and frequency of a sinusoid in the presence of harmonics/inter harmonics and noise plays an important role in a wide variety of power system applications, like protection, control and state monitoring. With this objective, the paper presents a novel hybrid approach for the accurate estimation of dynamic power system frequency, phasor and in addition to suppressing the effect of harmonics/interharmonics and noise in the voltage and current signals. The algorithm assumes that the current during a fault occurring on a power system consists of a decaying dc component, and time variant fundamental and harmonic phasors. For accurate estimation of fundamental frequency, phasor, decaying dc and ac components in the fault current or voltage signal, the algorithm uses a quadratic polynomial signal model and a fuzzy adaptive ADALINE filter with a modified Gauss–Newton algorithm. Extensive study has been carried out to demonstrate the performance analysis and fast convergence characteristic of the proposed algorithm. The proposed method can also be implemented for accurate estimation of dynamic variations in the amplitude and phase angles of the harmonics and inter harmonics mixed with high noise conditions.

1. Introduction

Real-time dynamic state monitoring, state estimation and islanding detection. are essential for wide area monitoring, protection and control applications in power networks. Nonstationary sinusoids occur in electrical power networks due to the proliferation of power electronic equipments, computers and microcontrollers. Further the integration of renewable energy sources in the utility grid results in the generation of harmonics, interharmonics, and severe waveform distortions [1,2]. It is well known that the harmonics/interharmonics interfere with sensitive electronic equipments and cause undesired power loss, overheating, and frequent fuse blowing. Also the speed and accuracy of the estimation algorithms are adversely affected by the presence of harmonics/interharmonics and noise in the signal [3]. Thus, there is an utmost need of an algorithm which can be efficient for accurate real-time dynamic phasor estimation that plays an important role in the area of protection and control application in power networks.

In recent years a large number of techniques have been proposed for the estimation of the power network phasor and frequency accurately. The simplest way to estimate the frequency of a signal is to measure the time of its zero

* Corresponding author. Tel.: +91 674 2727336; fax: +91 674 2350642.
E-mail address: pkdash.india@gmail.com (P.K. Dash).

http://dx.doi.org/10.1016/j.measurement.2016.03.026
0263-2241/

crossing [4]. However, the voltage and current waveforms are usually distorted and noisy. Most of the digital relays adopt discrete Fourier Transform (DFT) like Full cycle DFT [5,6], and its modifications [7–9] for phasor estimation of the voltage and current signals. Although Fourier based algorithms are efficient in estimating phasors accurately for time invariant signals, their performance deteriorates for time varying signals contaminated with noise and harmonic distortions. Another widely used algorithm for signal parameter estimation is the least squares algorithm [10], which, however, suffers from higher computational overhead since it requires matrix inversion at every iteration. Other methods like, Prony analysis technique [11], Kalman filters [12,13] and weighted least squares method [14] are based on the nonlinear curve fitting techniques and therefore suffer from inaccuracies when the signal frequency deviates widely from its nominal value. Parametric approaches [15], ESPRIT method [16], Improved Prony method [17], Fourier analysis [18], window based methods [19], are able to compute damping coefficients, but they are highly sensitive to noise and computationally expensive due to the finding of roots of higher order polynomials. Methods like orthogonal filtering [20], Taylor series expansion [21], wavelet transform [22,23], adaptive notch filter [24], Filter bank approach [25] require dedicated filters for removal of harmonic components before applying the algorithms for signal parameter estimation. Comparison of different adaptive algorithms for frequency and phasor estimation are provided in [26].

In recent years, artificial neural network based techniques [27,28] have been used for fundamental and harmonic phasor estimation due to their simplicity in structure and ease of computation in comparison to other well known techniques. Further the adaptive linear neuron known as ADALINE [29–31] has been used widely as a powerful tool for signal parameter estimation. But the conventional ADALINE was used for single output systems with tracking error, introduced due to non-stationary nature of the signal. Further, the arbitrary choice of the weights connecting the inputs to the computing neurons of the ADALINE gives rise to different tracking performance. A two-stage ADALINE discussed in [32] is capable of estimating fundamental frequency and phasor of a time varying signal under frequency deviation conditions but its computational cost is very high. In addition to this Fuzzy Logic and Neural network approaches have been employed for nonlinear systems including the power system applications, MIMO [33–35], SISO [36,37] and aerospace applications [38] where the state variables are difficult to be measured. Also to achieve wider operating conditions under uncertainties and to adopt to the nonlinear uncertainties Fuzzy Control has been used in [39,40] which emphasize the applicability of Fuzzy control to power system applications

Hence this paper proposes a hybrid approach for estimating the time varying amplitude, phase, and frequency of a sinusoid during fault condition to deal with time varying signal waveforms subjected to amplitude modulation, phase modulation, step change, and fundamental frequency deviations. Generally in case of a power network faults, the voltage and current signals comprise decaying dc and fundamental components and hence in the proposed approach they have been expressed as a time series using Taylor series expansion. The parameters of the expanded Taylor series are computed using the fuzzy variable step size ADALINE (FVSS ADALINE) where the learning parameters are made adaptive to compel the resultant error of the desired and estimated output to satisfy a stable difference error equation. As a result this approach, allows one to achieve better accuracy on the rate of convergence and stability by suitable selection of parameters of the error difference equation. The FVSS ADALINE approach is proposed for frequency estimation of time varying power signals and the modified recursive Gauss–Newton approach is used for phasor estimation [41,42] This hybrid approach using the quadratic polynomial signal model performs very well in terms of accuracy for signals with dynamic variations. In case of fast changes in signal dynamics, a new adaptive fuzzy logic based approach is proposed in this paper to update the step size of the ADALINE and cope up with the abrupt large and small deviations thereby providing significant noise rejection and faster convergence. The modified recursive Gauss–Newton ADALINE used for phasor estimation has been simplified by Hessian matrix approximation and also the need for matrix inversion at every iteration. This procedure results in reducing the computational complexity of the algorithm and in addition it also exhibits accurate tracking results in non-stationary environment using the objective function for error minimization. Moreover as per the demand in some real power signal application scenarios both the frequency estimation using FVSS and phasor estimation using modified recursive Gauss–Newton algorithm (MRGNA) approach can proceed simultaneously in the same iteration to detect any change either in the amplitude, phase or frequency of the time varying signal. Further for a three phase power system application, a multi-output ADALINE structure is discussed for the simultaneous estimation of amplitude and phase angle of three-phase current and voltage signals. A detailed study of the global convergence of the proposed FVSS ADALINE approach is presented in this paper. Extensive simulations are carried out to test the accuracy and speed of the proposed algorithm in various scenarios as observed in real power system applications. Simulation and experimental results show superiority of the proposed algorithm in estimating the dynamic behavior of the signal in presence of harmonic/interharmonic and noise over many conventional algorithms like DFT and ADALINE based methods.

The rest of the paper is organized as follows: Section 2 is divided into two parts, describing the proposed frequency and phasor estimation of the power signal, respectively. The performance analysis and global convergence characteristics of the proposed method are studied in Section 3 Numerous simulation and experimental results are presented in Section 4, while Section 5 outlines the conclusion.

2. Proposed algorithm

ADALINE based methods show inaccuracy in estimating fundamental frequency deviations in the presence of harmonics or interharmonics. The proposed algorithm is based on the Taylor series expansion to handle the dynamic behavior of the signal and its parameters are estimated using the modified ADALINE and Fuzzy variable step size ADALINE to yield the frequency and other signal parameters. The weight vector of the modified ADALINE is updated using a fast decoupled Gauss–Newton approach. The basic advantage of using ADALINE is its simple structure and ease of implementation. The authors [32] have proposed a two stage approach to ADALINE and have used RLS algorithm that requires the matrix inversion Lemma, increasing the computational cost of the algorithm. The computation time of the 2-stage ADALINE is significantly higher because of the use of Prony's method for frequency estimation, requiring 2M data samples to fit into M frequencies. In comparison to the two-stage ADALINE approach, this paper develops a frequency estimation method based on Taylor series expansion to model the dynamic signal using a quadratic polynomial where the Taylor coefficients are computed using the fuzzy variable step size ADALINE and the modified Gauss–Newton method is used for phasor estimation, which is based on the computation of a decoupled Hessian matrix. The hybrid approach results in a significant reduction of computational overhead in comparison to other available methods.

2.1. Frequency estimation

Let the discrete time dynamic signal, with changing amplitude, phase, and decaying dc component is modeled as

$$y(k) = A_{dc}e^{-kdt/\alpha} + \sum_{m=1}^{M} A_m(k)\sin(2\pi m f_0 kdt + \varphi_m(k)) \tag{1}$$

where $A_m(k)$ and $\varphi_m(k)$ are the time varying amplitude and phase angle of mth harmonic component, and f_0 is the nominal frequency of the signal, A_{dc} and α are the amplitude and time constant of decaying dc component, dt is the sampling time, M is the maximum order of the harmonic present in the signal. The total angle of the signal is $\theta_m(k) = 2\pi f_m kdt + \varphi_m(k)$. The frequency is taken as the rate of change of total angle θ_m [43].

The signal $y(k)$ in (1) is modeled as

$$\begin{aligned} y(k) = A_{dc}e^{-kdt/\alpha} &+ \sum_{m=1}^{M} A_m(k)\cos(\varphi_m(k)) \\ &\times \sin(2\pi m f_0 kdt) + A_m(k)\sin(\varphi_m(k)) \\ &\times \cos(2\pi m f_0 kdt) \end{aligned} \tag{2}$$

and further it can be represented as

$$\begin{aligned} y(k) = A_{dc}e^{-kdt/\alpha} &+ \sum_{m=1}^{M} f_{Cm}(k)\sin(2\pi m f_0 kdt) + f_{Sm}(k) \\ &\times \cos(2\pi m f_0 kdt) \end{aligned} \tag{3}$$

where $f_{Cm}(k) = A_m(k)\cos(\varphi_m(k))$, and $f_{Sm}(k) = A_m(k)\sin(\varphi_m(k))$. The time varying parameters $f_{Cm}(k)$ and $f_{Sm}(k)$ are expanded with second order Taylor series model, and we get

$$f_{Cm}(k) = a_{m0} + a_{m1}k + a_{m2}k^2, \quad f_{Sm}(k) = b_{m0} + b_{m1}k + b_{m2}k^2 \tag{4}$$

Neglecting the higher order terms, coefficients of the Taylor series expansion can be computed by taking the zero order, first order and second order derivatives respectively. The zero order derivative is given by

$$\begin{aligned} f_{Cm}(0) = a_{m0} = A_m(0)\cos(\varphi_m(0)) \quad \text{and} \quad f_{Sm}(0) = b_{m0} \\ = A_m(0)\sin(\varphi_m(0)) \end{aligned} \tag{5}$$

and for frequency estimation, the first order derivative is computed as

$$\begin{aligned} f'_{Cm}(0) &= a_{m1} = A'_m(0)\cos(\varphi(0)) - A_m(0)\varphi'(0)\sin(\varphi(0)), \\ &\text{and} \quad f'_{Sm}(0) = b_{m1} = A'_m(0)\sin(\varphi(0)) \\ &+ A_m(0)\varphi'(0)\cos(\varphi(0)) \end{aligned} \tag{6}$$

Using (5) and (6) and neglecting $A'_m(0)$, φ'_m is computed as

$$\varphi'_m(0) = \frac{a_{m0}b_{m1} - a_{m1}b_{m0}}{a_{m0}^2 + b_{m0}^2} \tag{7}$$

and from (7), the frequency of mth harmonic component is obtained as

$$\hat{f}_m = \tilde{f}_m + \varphi'_m(k)/2\pi dt = \tilde{f}_m + \frac{1}{2\pi dt}\cdot\frac{a_{m0}b_{m1} - a_{m1}b_{m0}}{a_{m0}^2 + b_{m0}^2} \tag{8}$$

$\tilde{f}_m$ is the initial estimate of the frequency. In the proposed method the coefficients of the Taylor series expansion for frequency estimation are obtained first by applying a modified ADALINE method to the voltage or current signal samples. For fundamental parameter estimation, the nonstationary voltage signal with a dc offset is modeled as

$$y(k) = A_{dc}e^{-kdt/\alpha} + A(k)\sin(2\pi f_0 kdt + \varphi(k)) \tag{9}$$

and the Taylor series expansion of the above signal is obtained as

$$\begin{aligned} y(k) = A_{dc}e^{-kdt/\alpha} &+ \left(a_0 + a_1k + a_2k^2\right)\sin(2\pi f_0 kdt) \\ &+ \left(b_0 + b_1k + b_2k^2\right)\cos(2\pi f_0 kdt) \end{aligned} \tag{10}$$

which can be represented in modified ADALINE as

$$y(k) = z(k)\cdot X^T(k) \tag{11}$$

where the coefficient vector is given as

$$z(k) = [a_0 \quad a_1 \quad a_2 \quad b_0 \quad b_1 \quad b_2] \tag{12}$$

and the sampled input vector is shown in (13)

$$X(k) = \begin{bmatrix} \sin(2\pi f_0 kdt) & kdt\sin(2\pi f_0 kdt) & (kdt)^2\sin(2\pi f_0 kdt) \\ \cos(2\pi f_0 kdt) & kdt\cos(2\pi f_0 kdt) & (kdt)^2\cos(2\pi f_0 kdt) \end{bmatrix} \tag{13}$$

The error signal used in weight vector update rule for the ADALINE is expressed as

$$e(k) = y(k) - z(k)\cdot X^T(k) \tag{14}$$

and the weight vector is updated using (15) as

$$z(k+1) = z(k) + \lambda\tanh(0.5^* e(k))^* X(k)/X(k)^* X^T(k) \tag{15}$$

where λ is the learning rate. Conventional ADALINE is simple, stable and fewer computations are required, but learning parameter needs to be tuned.

Another approach is discussed here for updating the weight vector of the ADALINE with variable step size [44]. When the estimation error is large, learning parameter is made large for faster tracking purposes, while for low estimation error, a small learning parameter is used for accurate estimation. Hence the learning parameter is made adaptive as follows:

The weight vector of the variable step size ADALINE is updated as

$$z(k+1) = \beta(k)z(k) + \lambda(k)e(k)X(k)/X(k)^{*}X^{T}(k) \quad (16)$$

where $\beta(k) = e^{\lambda^{r}(k)}$, and the learning rate is varied as

$$\lambda(k) = \alpha\, a\tan(c|e(k)e(k-1)|) + \gamma\lambda(k-1) \quad (17)$$

The above algorithm provides better convergence rate in adaptive systems. It has been tested with sigmoid function and hyperbolic tangent function as in [45]. In this method error covariance is used to adjust the step size. This method eliminates sensitivity to noise and is suitable only for slow changes in signal parameters. Thus for fast changes in signal parameters, a new fuzzy logic based approach is proposed in this paper to update the step size of the ADALINE. The proposed fuzzy model is described below:

The variable step size learning rate is expressed as

$$\lambda(k) = \lambda(k-1) + \Delta\lambda \quad (18)$$

where change in step size $\Delta\lambda$ is updated using a simple Fuzzy rule base and Fuzzy membership values. The proper selection of membership function is a core issue in fuzzy control. In the proposed model, the Fuzzy membership values are chosen as functions of the standard deviation δ. When the deviation is large in the initial period or there is any change in the system parameters, the step size should be large for better convergence and tractability. On the other hand when the deviation is small after the algorithm has converged, the step size should also be adapted accordingly. Hence the change in standard deviation is computed as

$$\Delta\delta = e^{2}(k) - e^{2}(k-1) \quad (19)$$

and the Fuzzy rule base for arriving at a change in step size is represented as follows:

R1. If $|\Delta\delta|$ is Large Then $\Delta\lambda = \mu_{L}K_{1}\Delta\delta$ (20)

R2. If $|\Delta\delta|$ is Small Then $\Delta\lambda = \mu_{S}K_{2}\Delta\delta$ (21)

where the membership functions for Large and Small are given by

$$\mu_{L}(\Delta\delta) = 1 - \exp^{-|\Delta\delta|}, \quad \text{and} \quad \mu_{S}(\Delta\delta) = \exp^{-|\Delta\delta|} \quad (22)$$

where K_1 and K_2 are small positive numbers between 0 and 1, and $0 \leqslant |\Delta\delta| \leqslant 1$.

Using centroid defuzzification principle, the value of $\Delta\lambda$ is obtained as

$$\Delta\lambda = \frac{\mu_{L}K_{1}\Delta\delta + \mu_{S}K_{2}\Delta\delta}{\mu_{S} + \mu_{L}} \quad (23)$$

and the weight vector of the ADALINE is updated using (16) as

$$\begin{aligned} a_0(k+1) &= \beta(k)a_0(k) + \lambda(k)e(k)\sin(2\pi f_0 kdt)/\sin^2(2\pi f_0 kdt) \\ a_1(k+1) &= \beta(k)a_1(k) + \lambda(k)e(k)\sin(2\pi f_0 kdt)/(kdt)\sin^2(2\pi f_0 kdt) \\ a_2(k+1) &= \beta(k)a_2(k) + \lambda(k)e(k)\sin(2\pi f_0 kdt)/(kdt)^2\sin^2(2\pi f_0 kdt) \end{aligned} \quad (24)$$

Similarly

$$\begin{aligned} b_0(k+1) &= \beta(k)b_0(k) + \lambda(k)e(k)\cos(2\pi f_0 kdt)/\cos^2(2\pi f_0 kdt) \\ b_1(k+1) &= \beta(k)b_1(k) + \lambda(k)e(k)\cos(2\pi f_0 kdt)/(kdt)\cos^2(2\pi f_0 kdt) \\ b_2(k+1) &= \beta(k)b_2(k) + \lambda(k)e(k)\cos(2\pi f_0 kdt)/(kdt)^2\cos^2(2\pi f_0 kdt) \end{aligned} \quad (25)$$

The frequency of the signal is estimated as

$$\hat{f}_0 = \widetilde{f}_0 + \varphi'(k)/2\pi dt = \widetilde{f}_0 + \frac{1}{2\pi dt}\cdot\frac{a_0 b_1 - a_1 b_0}{a_0^2 + b_0^2} \quad (26)$$

To verify the performance of the proposed fuzzy variable step size ADALINE, a function between error signal $e(k)$ and step size $\lambda(k)$ is formulated. In the initial iterations, the weight deviates from the optimal value, and $e(k)$ is large, so $\lambda(k)$ should also be large for faster convergence. Hence a plot between $e(k)$ and $\lambda(k)$ is taken for different algorithms with a view for comparison. From Fig. 1 we can observe that the hyperbolic tangent function produces singularity when error is near to 0 and thus a small change in error produces large change in weight vector. Although the arc-tangent function shows some improvement, the proposed algorithm is found to be superior as it exhibits a very smooth transition between the change in error and step size providing a better convergence speed to the algorithm. Moreover the function plot for the proposed method between the error signal $e(k)$ and step size $\lambda(k)$ reveals that in the initial phase when the error is high, $\lambda(k)$ is high for faster rate of convergence but subsequently when the algorithm achieves a steady state and the error reduces to the lowest value, $\lambda(k)$ also attains its minimal value thereby achieving the optimal wiener value.

2.2. Phasor estimation

In this section the amplitude and phase of the nonstationary signal along with decaying dc component are estimated using the ADALINE approach with the weights updated through a modified Gauss–Newton algorithm. The modified Gauss–Newton algorithm has the basic advantage of eliminating the need for matrix inverse at every iteration, which results in reducing the computational overhead of the algorithm. The estimated frequency in section A is used to estimate the amplitude and phase of the signal in the same iteration. Let the discrete time signal is represented as:

$$\hat{y}(k) = \hat{A}_{dc}e^{-kdt/\hat{\alpha}} + \sum_{m=1}^{M}\hat{A}_m(k)\sin(2\pi\hat{f}_m kdt + \hat{\varphi}_m(k)) \quad (27)$$

where $\hat{f}_m$ is the frequency estimated using Eq. (8). The fundamental signal with decaying dc component is decomposed as

$$\hat{y}(k) = \hat{A}_{dc}e^{-kdt/\hat{\alpha}} + \hat{A}(k)\cos(\hat{\varphi}(k))\sin(2\pi\hat{f}kdt) + \hat{A}(k) \times \sin(\hat{\varphi}(k))\cos(2\pi\hat{f}kdt) \quad (28)$$

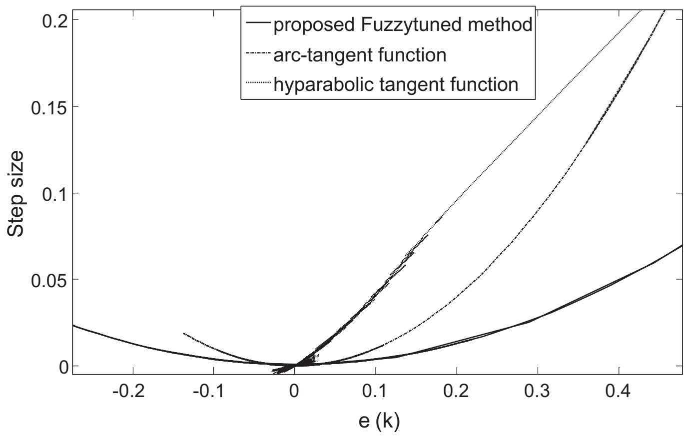

Fig. 1. Proposed method —, hyperbolic tangent function --- arc tan function –·–·–.

where $e^{-kdt/\alpha}$ is expanded using Taylor series expansion as

$$e^{-kdt/\alpha} = 1 - \frac{kdt}{\alpha} + \frac{1}{2!}\left(\frac{kdt}{\alpha}\right)^2 - \ldots\ldots$$

Neglecting the higher order terms of Taylor series expansion the signal is represented as

$$\hat{y}(k) = w_1 + w_2 kdt + w_3 \sin(2\pi\hat{f}kdt) + w_4 \cos(2\pi\hat{f}kdt) \quad (29)$$

where $w_1 = A_{dc}$, $w_2 = -A_{dc}(1/\alpha)$, $w_3 = \hat{A}(k)\cos(\hat{\varphi}(k))$ and $w_4 = \hat{A}(k)\sin(\hat{\varphi}(k))$ and the signal is represented in vector form as

$$\hat{y}(k) = W(k) \cdot X^T(k) \quad (30)$$

where the coefficient vector and the state vector are given as

$$W(k) = [w_1\ w_2\ w_3\ w_4],$$
$$X(k) = \left[1\ kdt\ \sin(2\pi\hat{f}kdt)\ \cos(2\pi\hat{f}kdt)\right] \quad (31)$$

and the coefficient vector of the ADALINE is updated using modified Gauss–Newton algorithm for better accuracy in estimation and less computation in comparison to the RLS approach [46].

An exponential weighted error cost function is used for updating the coefficients as follows:

$$H(k) = \sum_{i=0}^{k} \eta^{k-i} \begin{bmatrix} 1 & kdt & \sin(2\pi\hat{f}kdt) & \cos(2\pi\hat{f}kdt) \\ kdt & (kdt)^2 & kdt\sin(2\pi\hat{f}kdt) & kdt\ \cos(2\pi\hat{f}kdt) \\ \sin(2\pi\hat{f}kdt) & kdt\sin(2\pi\hat{f}kdt) & \sin^2(2\pi\hat{f}kdt) & \sin(2\pi\hat{f}kdt)\cos(2\pi\hat{f}kdt) \\ \cos(2\pi\hat{f}kdt) & kdt\cos(2\pi\hat{f}kdt) & \sin(2\pi\hat{f}kdt)\cos(2\pi\hat{f}kdt) & \cos^2(2\pi\hat{f}kdt) \end{bmatrix} \quad (37)$$

$$\varepsilon(k) = \sum_{i=0}^{k} \eta^{k-i} e_j^2(i), \quad \text{with } 0 < \eta \leqslant 1 \quad (32)$$

where the a priori estimation error is given as

$$e_j(k) = y(k) - W(k) \cdot X^T(k) \quad (33)$$

where η is a forgetting factor in general taking up values within $0 < \eta \leqslant 1$ (practically 0.5) which is responsible for deciding the rate of convergence and accuracy of the algorithm. This formulation of the exponential weighted error cost function assigns higher weightage to the immediate past errors and lesser weight to past errors, as the forgetting factor is assigned with higher powers for the past errors. The modified Gauss–Newton method is used to minimize the exponential weighted error cost function given in (32). The coefficients are updated as follows:

$$\widetilde{W}(k) = \widetilde{W}(k-1) - H^{-1}(k)\psi(k)e_j(k) \quad (34)$$

$$\text{where } H(k) = \sum_{i=0}^{k} \eta^{k-i} \psi(i)\psi^T(i) \quad (35)$$

and the gradient vector ψ is obtained as:

$$\psi(k) = \frac{\partial e_j(k)}{\partial \widetilde{W}} = \begin{bmatrix} -1 \\ -kdt \\ \sin(2\pi\hat{f}kdt) \\ \cos(2\pi\hat{f}kdt) \end{bmatrix} \quad (36)$$

The Hessian matrix $H(k)$ can be written as:

To compute $H^{-1}(k)$ one can directly use the matrix inverse lemma as in RLS [46], which is computationally expensive. Thus to reduce the computational complexity and increase the speed, the Hessian matrix is approximated by using an assumption that $2\pi\hat{f}$ is not near to 0 or π as

$$H(k) = \sum_{i=0}^{k} \eta^{k-i} \begin{bmatrix} 1 & 0 & 0 & 0 \\ 0 & \sum_{i=1}^{k-1} (idt)^2 \eta^{k-i} & 0 & 0 \\ 0 & 0 & 1/2 & 0 \\ 0 & 0 & 0 & 1/2 \end{bmatrix} \tag{38}$$

where we can approximate the following function as

$$\sum_{i=0}^{k} i^2 \eta^{k-i} \approx \frac{1}{k} \frac{(k+1)(2k+1)}{6} k \sum_{0}^{k} \eta^{k-i}$$

and $H(k)$ can be written as

$$H(k) = \frac{1-\eta^{k+1}}{2(1-\eta)} \begin{bmatrix} 2 & 0 & 0 & 0 \\ 0 & \frac{(dt)^2(k+1)(2k+1)}{6} \sum_{0}^{k} \eta^{k-i} & 0 & 0 \\ 0 & 0 & 1 & 0 \\ 0 & 0 & 0 & 1 \end{bmatrix} \tag{39}$$

and the inverse $H^{-1}(k)$ is computed as:

$$H^{-1}(k) = \begin{bmatrix} \frac{2}{C(k)} & 0 & 0 & 0 \\ 0 & \frac{12(k+1)}{C(k)G_{\varphi}(k)(dt)^2} & 0 & 0 \\ 0 & 0 & \frac{1}{C(k)} & 0 \\ 0 & 0 & 0 & \frac{1}{C(k)} \end{bmatrix} \tag{40}$$

$$\text{where } c(k) = \frac{1-\eta^{k+1}}{2(1-\eta)} = \quad \text{and} \quad G_{\varphi}(k) = k^2 + 12\,k - 1 \tag{41}$$

It can also be observed that $c(k)$ and $G_{\varphi}(k)$ can be updated iteratively as

$$c(k) = \eta c(k-1) + 1/2, \quad \text{and} \quad G_{\varphi}(k) = G_{\varphi}(k-1) + 2k + 11 \tag{42}$$

Further by putting (40) and (41) into (34) the following update equations are obtained:

$$\tilde{w}_1(k+1) = \tilde{w}_1(k) + 2e_j(k)/c(k) \tag{43}$$

$$\tilde{w}_2(k+1) = \tilde{w}_2(k) + 12\,k\,(k+1)\,e_j(k)/dt\,c(k)\,G_{\phi} \tag{44}$$

$$\tilde{w}_3(k+1) = \tilde{w}_3(k) + \sin(2\pi\hat{f}kdt)e_j(k)/c(k) \tag{45}$$

$$\tilde{w}_4(k+1) = \tilde{w}_4(k) + \cos(2\pi\hat{f}kdt)e_j(k)/c(k) \tag{46}$$

and the dynamic amplitude, phase, decaying dc component and the time constant of the dc component of the signal are estimated using Eqs. (43)–(46) as follows:

$$\hat{A}_{dc}(k) = \hat{A}_{dc}(k-1) + \frac{2e_j(k)}{J(k)} \tag{47}$$

$$\hat{\alpha}(k) = -w_1(k)/w_2(k) \tag{48}$$

$$\hat{A}(k) = \sqrt{\tilde{w}_3(k+1)^2 + \tilde{w}_4(k+1)^2} \tag{49}$$

$$\hat{\phi}(k+1) = \arctan(\tilde{w}_4(k+1)/\tilde{w}_3(k+1)) \tag{50}$$

Hence, the above equations provide a simplified expression for estimating the fundamental and the dc component of a signal. It can easily be expanded for harmonic/interharmonic estimation too. From the above equations it is clear that the estimation accuracy of the parameters depend on the learning rate η which can be updated using a Fuzzy rule base tuning approach in a manner similar to λ as in the previous section.

3. Performance analysis

To study the performance analysis of the proposed Fuzzy variable step size algorithm, we will first analyze the sensitivity of the proposed algorithm to noise under stationary condition. The error signal is described as

$$e(k) = y(k) - X^T(k)z(k) \tag{51}$$

$$\text{or } y(k) = e(k) + X^T(k)z(k) \tag{52}$$

where the desired signal can be considered as

$$y(k) = \varsigma(k) + X^T(k)z^* \tag{53}$$

where $\varsigma(k)$ is a zero mean white Gaussian independent distribution, and z^* is the optimal weight vector. Hence substituting (52) and (53) we get

$$e(k) = \varsigma(k) - X^T(k)[z(k) - z^*] = \varsigma(k) - X^T(k)\Delta(k) \tag{54}$$

where $\Delta(k) = z(k) - z^*$.

The proposed algorithm uses change in standard deviation to formulate the Fuzzy rule base, hence the expectation of the autocorrelation between $e(k)$ and $e(k-1)$ is studied. Thus

$$\begin{aligned} E[e(k)e(k-1)] = E[&\varsigma(k)\varsigma^T(k-1) - \varsigma(k)X^T(k-1)\Delta(k-1) \\ &- \Delta(k)X^T(k)\varsigma(k-1) \\ &+ \Delta(k)X(k)X^T(k-1)\Delta(k-1)] \end{aligned} \tag{55}$$

as $\varsigma(k)$ is a zero mean white Gaussian distribution and is independent, (55) can be rewritten as

$$E[e(k)e(k-1)] = E[\Delta(k)X(k)X^T(k-1)\Delta(k-1)] \tag{56}$$

Hence it can be observed that the correlation of the error signal is independent of the noise distribution eliminates sensitivity to noise.

Now assume the Lyapunov function [31] as:

$$\upsilon(k) = z^T(k)R^{-1}(k)z(k) \tag{57}$$

$$\text{where } R(k) = E[X(k)X^T(k)] \tag{58}$$

and by taking the diagonal elements of the matrix as:

$$X(k)X^T(k) = trR \tag{59}$$

Eq. (57) can be written as

$$\begin{aligned} &\upsilon(k)z^{-1}(k)X(k)X^T(k)X(k) = z^T(k)X(k) \\ &\upsilon(k)\,trR\,z^{-1}(k)X(k) = z^T(k)X(k) \end{aligned} \tag{60}$$

$$\text{or } v(k) = \frac{1}{trR} z^T(k) z(k) \quad (61)$$

Again the weight vector of fuzzy variable step size ADALINE is updated as

$$z(k) = \beta z(k-1) + \lambda(k-1)e(k-1)X(k-1)/X(k-1)X^T(k-1) \quad (62)$$

Further the Lyapunov function can be written as

$$v(k) = \frac{1}{trR}[\beta z^T(k-1) + \lambda(k-1)e(k-1)X^T(k-1)/X^T(k-1)X(k-1)]^* [\beta z(k-1) + \lambda(k-1)e(k-1)X(k-1)/X(k-1)X^T(k-1)] \quad (63)$$

$$\begin{aligned} \text{or } v(k) = \frac{1}{trR}[&\beta z^T(k-1)z(k-1) \\ &+ \beta z^T(k-1)\lambda(k-1)e(k-1)X(k-1) \\ &/X(k-1)X^T(k-1) + \beta z(k-1)\lambda(k-1)e(k-1)X^T(k-1) \\ &/X^T(k-1)X(k-1) + \lambda^2(k-1)e^2(k-1)X^T(k-1)X(k-1) \\ &/X^T(k-1)X(k-1)X(k-1)X^T(k-1)] \end{aligned} \quad (64)$$

which can further be simplified to

$$\begin{aligned} v(k) = &\beta^2 v(k-1) + \lambda^2(k-1)e^2(k-1) \\ &+ (2\beta/trR)z(k-1)\lambda(k-1)e(k-1)X(k-1) \\ &/X^T(k-1)X(k-1) \end{aligned} \quad (65)$$

as $\Delta(k) = z(k) - z^*$ and $e(k) = -X^T(k)\Delta(k)$

hence we can further simplify (65) as

$$\begin{aligned} v(k) = &\beta^2 v(k-1) \\ &- \frac{2\beta}{trR} z(k-1)\lambda(k-1)X^T(k-1)X(k-1)\Delta^T(k-1) \\ &+ \lambda^2(k-1)X^T(k-1)\Delta^T(k-1)X(k-1)\Delta(k-1) \\ v(k) = &\beta^2 v(k-1) - \frac{2\beta}{trR}\lambda(k-1)\Delta^T(k-1)Rz(k-1) \\ &+ \lambda^2(k-1)\Delta^T(k-1)R\Delta(k-1) \end{aligned} \quad (66)$$

On simplification the following result is obtained:

$$\begin{aligned} \beta^2 v(k-1) - v(k) = &\frac{2\beta}{trR}\lambda(k-1)\Delta^T(k-1)Rz(k-1) \\ &- \lambda^2(k-1)\Delta^T(k-1)R\Delta(k-1) \end{aligned} \quad (67)$$

By assuming $\beta \cong 1$

$$v(0) - v(k) = \sum_{i=0}^{k-1} \frac{2}{trR}\lambda(i)\Delta^T(i) R [z(i) - 2\lambda(i) trR \Delta(i)] \quad (68)$$

as $\lim_{i\to\infty}\Delta(i) \to 0$ the value of (68) is limited. Hence

$$\lim_{i\to\infty} 2\lambda(i)\Delta^T(i)R/trR[z(i) - 2\lambda(i)trR\Delta(i)] = 0$$

as (69)

$$z(i) - 2\lambda(i)trR\Delta(i) \neq 0,\ \lambda(i) \neq 0,\ R \neq 0$$

then as

$$\Delta(i) = z(i) - z^* \quad \text{and} \quad \lim_{i\to\infty} z(i) = z^* \quad (70)$$

Using (61) we can generate

$$\dot{v}(k) = \frac{2}{trR} z^T(k)\frac{\Delta z(k)}{\Delta\tau}$$

$$\text{or } \dot{v}(k) = \frac{2}{trR} z^T(k)\dot{z}^T(k) \quad (71)$$

or using (67) $\dot{v}(k)$ can be written as

$$\dot{v}(k) = \frac{2\beta\lambda(k-1)\Delta^T(k-1)R}{\Delta\tau trR}[2\lambda(k-1)trR\Delta(k-1) - z(k-1)] \quad (72)$$

Now using (71) and (72)

$$\begin{aligned} &2\beta\lambda^2(k-1)\Delta^T(k-1)RtrR\Delta(k-1) \\ &= z(k)\Delta z(k) + \beta\lambda(k-1)\Delta^T(k-1)Rz(k-1) \end{aligned} \quad (73)$$

and as $\lim_{k\to\infty}\Delta(k) = 0$, and $z(k) \neq 0$

hence we get

$$\lim_{k\to\infty}\Delta z(k) = \lim_{k\to\infty}[z(k) - z(k-1)] = 0 \quad (74)$$

This demonstrates the global convergence of the proposed Fuzzy variable step size ADALINE.

4. Performance evaluation

A wide variety of computer simulations has been carried out first to evaluate the performance of the proposed algorithm in estimating amplitude, phase and frequency under stationary, dynamic, transient and noisy conditions. For ADALINE based algorithms, all the weights are initialized to zero values. The test signal is sampled at a rate of 5 kHz (100 samples per cycle). Further to evaluate the performance of the proposed algorithm in a laboratory setup, voltage and current signals are generated using transient condition in Matlab/Simulink environment, and tested for 3-phase system.

4.1. Using computer simulated signal

4.1.1. Case I: noise test

The sinusoidal test signal is first verified for the noise rejection ability of the proposed algorithm. The signal model of a static sinusoid is used for this case, and is represented as

$$y(k) = A(k)\sin(2\pi f_0 kdt + \varphi(k)) + v(k) \quad (75)$$

where A = 1.2 p.u, f_0 = 60 Hz and φ = 0.6 rad. The test signal given in Eq. (75) is added with zero-mean white Gaussian noise $v(k)$. The signal is tested under various noise conditions and the mean square estimation error in dB for different algorithms is shown in Fig. 2. Algorithms like, RDFT [8], Least squares [10], ADALINE [29], and the proposed method are considered for comparison.

The superior performance of the proposed algorithm over different algorithms can clearly be observed from the above convergence curve. From the convergence curve of the proposed method in Fig. 2, it can be concluded that the mean square estimation error in dB is in a very small range which further decreases as the SNR value of the noise increases as compared to other standard approaches. Further the computational complexity of the proposed algorithm for fundamental component estimation at each iteration is compared with algorithms like Two stage ADALINE [32] and RGN [47]. As shown in Table 1 the number of

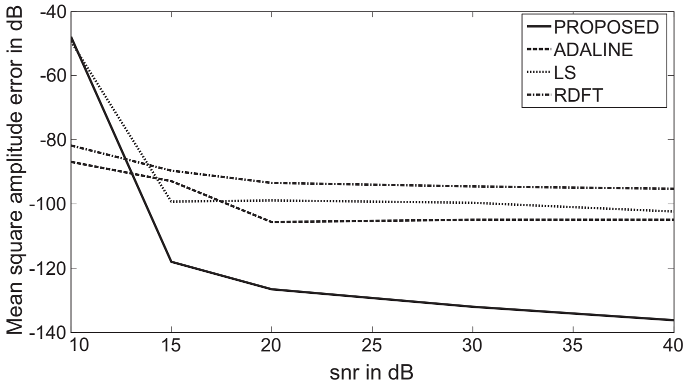

Fig. 2a. Mean square amplitude error in dB at different noise level.

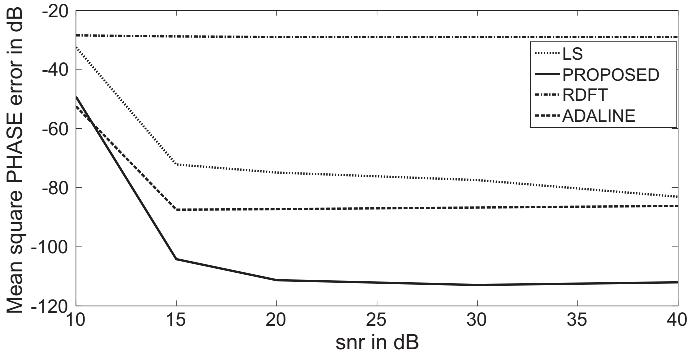

Fig. 2b. Mean square phase error in dB at different noise level.

Table 1
Computational requirements of different algorithms.

Algorithm	Multiplication/division
Two stage ADALINE	52
RGN	42
Proposed method	28

computations required are very high in the Two stage ADALINE method because of the matrix inversion required at every iteration, which have been reduced in the proposed algorithm by Hessian matrix approximation.

4.2. Dynamic signal test

4.2.1. Case II: estimation of modulated power signals

The amplitudes of the voltage and current signals are modulated with a low frequency signal during power swing. In this case the envelope of the fundamental voltage signal going through step and modulated changes is shown. The test signal in (75) goes through the following changes:

$$
\begin{aligned}
y(k) &= \sin(2\pi f_0 kdt);\ \text{for } k < 100 \\
y(k) &= 0.9^* \sin(2\pi f_0 kdt);\ \text{for } 100 \leqslant k < 300 \\
y(k) &= (1.2 + (0.1^* \sin(2\pi 15kdt) \\
&\quad + 0.05^* \sin(22\pi kdt)))^* \sin(2\pi f_0 kdt);\ \text{for } k \geqslant 300
\end{aligned} \tag{76}
$$

The performance of the proposed algorithm under dynamic behavior of the signal is compared with the ADALINE [29] based method. Fig. 3 shows better performance of the proposed algorithm over conventional ADALINE based signal parameter estimation approach. From Fig. 3 it is clear that the proposed algorithm converges to the true value and dynamically changes with time to cope the changing envelope of the signal. As observed from Fig. 3 the proposed approach is quite capable of tracking the fast changing signal envelope in less than a cycle unlike the conventional ADALINE approach which consumes considerably more samples to converge. For better comparison the test is performed 100 times and the mean of the RMSE at different noise level of different algorithms like EKF [12], LS [10], ADALINE [29], and the proposed method are depicted in Table 2. The superior performance of the proposed algorithm can easily be observed from this Table. The proposed method shows significantly better noise rejection capability as compared to the other conventional methods, even under extreme noise conditions of SNR = 20 dB, due to the fact that the proposed approach uses error covariance to adjust the step size which reduces sensitivity to noise.

4.2.2. Case III: performance evaluation in the presence of harmonics/interharmonics

In this case the inherent noise rejection ability of the proposed filter is studied due to the presence of harmonics

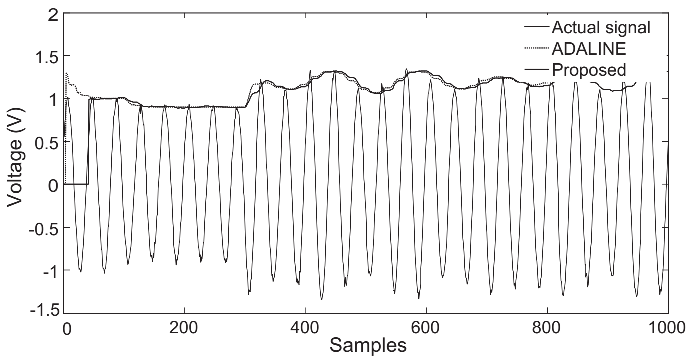

Fig. 3. Estimated envelope of the dynamic signal.

Table 2
RMSE at different noise level of different algorithms.

Property	EKF			LS			ADALINE			Proposed		
	20 dB	30 dB	40 dB	20 dB	30 dB	40 dB	20 dB	30 dB	40 dB	20 dB	30 dB	40 dB
Fundamental amplitude	0.1232	0.101	0.0511	0.1011	0.0914	0.0269	0.0763	0.0614	0.0588	0.0052	0.0032	0.0021
Frequency	0.0124	0.0095	0.0072	–	–	–	0.1536	0.1479	0.1325	0.0096	0.0084	0.0066
Dc offset	–	–	–	0.0076	0.0069	0.006	0.1037	0.0974	0.0935	0.0077	0.0056	0.0038

and interharmonics considered as noise. The test signal for this purpose is shown in Eq. (77):

$$y(k) = 1.2^{*}\sin(\omega_0 kdt + \varphi(k)) + 0.2^{*}\sin(3^{*}\omega_0 kdt + \varphi(k)) + 0.1^{*}\sin(5^{*}\omega_0 kdt + \varphi(k)) + 0.05\sin(7^{*}\omega_0 kdt + \varphi(k)) + 0.1\sin(\omega_{ih} kdt + \varphi(k)) \quad (77)$$

where the signal is corrupted with 16% third harmonic, 8% fifth harmonic, 4% seventh harmonic, fundamental frequency is 50 Hz and interharmonic frequency is 170 Hz. Fig. 4 shows the absolute estimation error of the proposed algorithm for different parameters. Table 3 summarizes the estimation error results for each harmonic and interharmonic contamination which are obtained by taking the mean over the 500 samples of the input signals. It can also be observed clearly from Fig. 4 that the proposed algorithm performs significantly well and a yields accurate result even under high percentage of harmonic contamination and thereby exhibits robust performance even in the presence of harmonic and interharmonic components as noise.

4.2.3. Case IV: magnitude, phase and frequency step test

In practical power system scenario switching, fault and tripping conditions introduce abrupt changes in magnitude, phase angle and frequency of the current or voltage signals. So in this case a similar situation is analyzed where all the signal parameters like amplitude, phase and frequency of the signal are suddenly changed and the step signal is contaminated with white Gaussian noise of SNR = 20 dB. The convergence of the proposed algorithm to the true value is tested. The signal in (75) is varied as mentioned in Table 4.

As a result of sudden change in all the parameters, it can be observed from Fig. 5 that not only the frequency converges to the true value in less than half a cycle but also shows smooth response during both the transitions of positive and negative steps (+−1 Hz), the amplitude and phase still take a little more settling time to converge i.e. half a cycle with some more samples. From the results it is observed that the proposed algorithm performs much better in tracking the signal parameters accurately during sudden changes of frequency, amplitude and phase angle in comparison to the conventional estimation techniques.

4.2.4. Case V: short circuit current test

To test the robustness and efficiency of the proposed filter for signals comprising both damped sinusoids and decaying dc components a practical situation involving distributed generation systems like doubly-fed wind turbine generators (DFIG) in a microgrid is considered in this paper. It is well known that the short-circuit current of a wind generating system is found to be a combination of an exponentially decaying dc component and time varying fundamental frequency component along with harmonics. The test signal, therefore, is represented as

$$y(k) = A_{dc}e^{-t/\alpha_1} + (A_{ac} + Ae^{-t/\alpha_2})^{*}\sin(\omega_0 kdt + \varphi(k)) + \sum_{i=3}^{5} A_i \sin(i\omega_0 kdt + \varphi_i(k))Ae^{-t/\alpha_2} \quad (78)$$

where A_{dc} and α_1 are amplitude and time constant of decaying dc component and A, A_{ac} and α_2 are the constant amplitude, decaying amplitude and time constant of the fundamental component. In this case the decaying dc and decaying ac amplitude of the fundamental component are kept equal to 1.0 pu, with decaying 3rd and 5th harmonic components. Fig. 6 shows that even in the presence

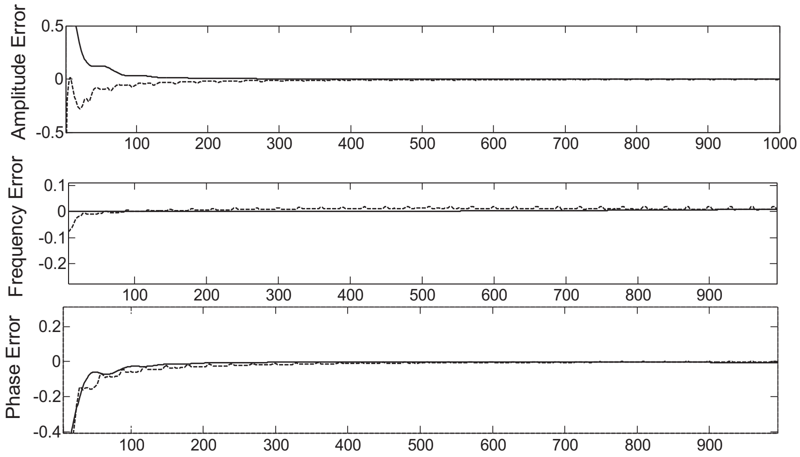

Fig. 4. Estimation error: without harmonic —, with harmonic as noise – – –.

Table 3
Estimation error results for each harmonic and interharmonic.

Parameters	Estimation error: without harmonic	Estimation error: with harmonic and interharmonic as noise			
		3rd harmonic	5th harmonic	7th harmonic	Interharmonic
Amplitude (p.u)	2.12e−007	3.12e−007	2.32e−005	5.82e−004	3.42e−002
Phase (rad)	3.01e−004	6.12e−003	5.56e−003	9.22e−002	5.44e−001
Frequency (Hz)	1.56e−005	4.46e−005	4.88e−003	2.64e−003	3.12e−002

Table 4
Variation of nonstationary signal parameters.

Time interval in samples					
Sample value	0–300	300–400	400–500	500–700	700–1000
Amplitude	1.2	1.5	1.5	1.5	1.2
Frequency	60	60	61	61	60
Phase	$\pi/6$	$\pi/6$	$\pi/6$	$\pi/5$	$\pi/6$

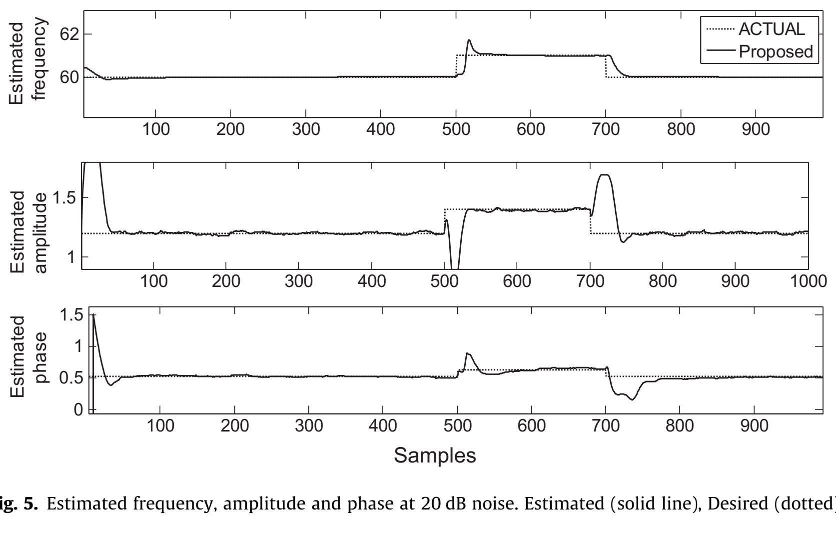

Fig. 5. Estimated frequency, amplitude and phase at 20 dB noise. Estimated (solid line), Desired (dotted).

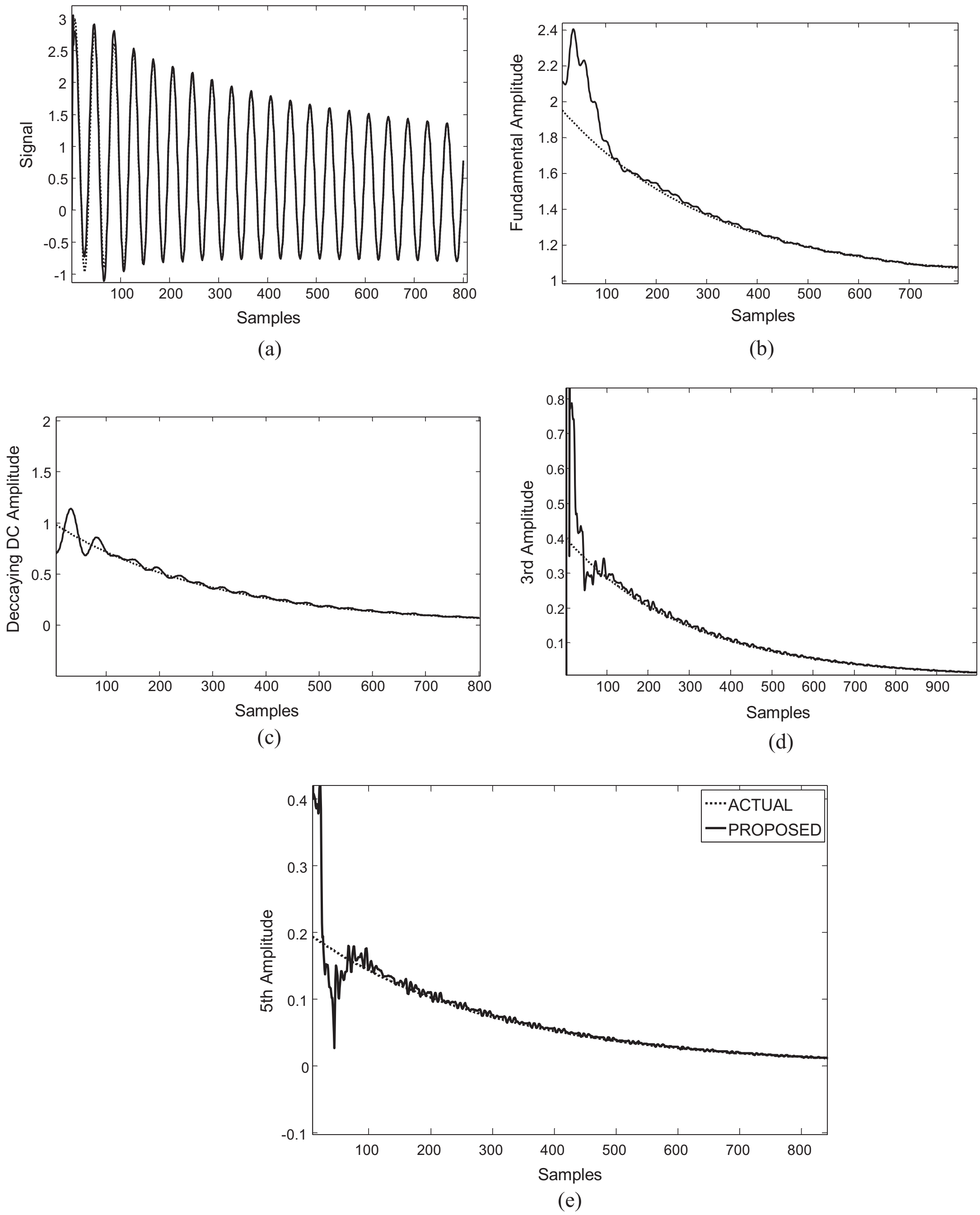

Fig. 6. (a) Actual and the estimated signal. (b) Actual and the estimated fundamental amplitude. (c) Actual and the estimated decaying dc amplitude. (d) Actual and the estimated 3rd harmonic amplitude. (e) Actual and the estimated 5th harmonic amplitude. Actual ….., proposed —.

of large decaying dc and decaying ac components, the algorithm is able to estimate the envelope accurately within one cycle of the 50 Hz waveform. The proposed algorithm exhibits fast tracking due to the fact that unlike the conventional Gauss–Newton approach, here there is no need to invert a Jacobian.

4.2.5. Case VI: modulated phasor with harmonics

In this case study a test signal with modulated amplitude and phase is considered. The 3rd and 5th harmonic components are injected into the signal after 15 cycles. The test signal used in this case is a critical case which exhibits dynamic variations due to amplitude modulation by high frequency components as well as phase modulation in the fundamental and harmonic components. The test signal is depicted in Eq. (79) as:

$$y(k) = a(k)\sin(2\pi f1k + \phi(k)) + u(k)\left[\frac{a(k)}{10}\sin(2\pi 3f1k) + \phi_3(k)) + \frac{a(k)}{20}\sin(2\pi 5f1k) + \phi_5(k))\right] \quad (79)$$

where

$$uk) = \begin{cases} 0, & \text{for } k < 15/f1 \\ 1, & \text{for } k \geqslant 15/f1 \end{cases}$$

$$a(k) = a1 + a11\sin(2\pi f_a k)$$

$$\phi(k) = \phi_0 + \phi_{11}\sin(2\pi f_\phi k)$$

$$\phi_3(k) = 0.9\phi(k)$$

$$\phi_5(k) = 0.8\phi(k)$$

with $a1 = 1$, $a11 = 0.2$, $\phi_0 = 1$, $\phi_{11} = 0.1$, $f_a = f_\phi = 5$ Hz.

Fig. 7 shows the ability of the proposed algorithm to track the phasor estimates present in the signal. It can be observed from the figure that the error is high at the time of harmonic injection and the estimation closely follows the ideal value and even converges to the true value within a cycle. The estimation results can be further improved by improving the frequency estimation results which is fed to the second stage for phasor estimation by considering a Taylor series model of higher orders in the FVSS approach.

4.2.6. Case VII: off nominal frequency with decaying dc components test

It is well known that the presence of unbalanced loads in a power network may cause the fundamental frequency to deviate from its nominal value. Further the fault current or voltage signal may also be contaminated by decaying dc components as well as may be confronted with off nominal frequency situation which makes the power signal more critical to be estimated. To test the estimation accuracy of the proposed algorithm during such a fault condition, the test signal is represented in the following way:

$$y(k) = \begin{cases} \sqrt{2}\sin[2\pi\cdot(50+\Delta f)k\cdot dt] & (k \leqslant 500) \\ 3\sqrt{2}\sin[2\pi\cdot(50+\Delta f)k\cdot dt] + e^{-n/0.05} & (k > 500) \end{cases} \quad (80)$$

where Δf is the frequency deviation, which is considered as 1.0 Hz and 2.0 Hz in two independent cases.

Fig. 8 shows the superior performance of the proposed algorithm under frequency deviation as well as decaying dc component. From the figure it is observed that the proposed approach exhibits less oscillation in case of amplitude estimation and also the convergence rate to the ideal value is quite fast (within half a cycle) in comparison to other standard approaches. It is due to the fact that the proposed approach considers both decaying D.C and dynamic characteristics. The magnitude estimation error of the proposed approach is also in a very small range which emphasizes the accuracy of the proposed approach

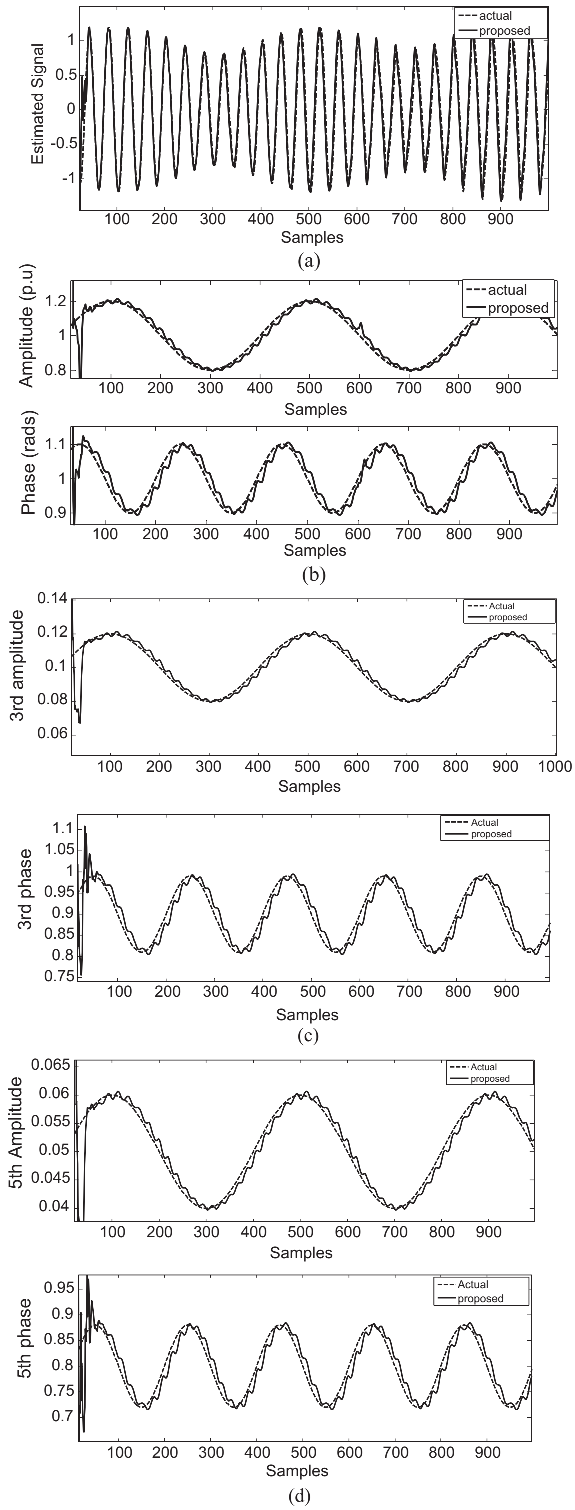

Fig. 7. (a) Actual and the estimated signal. (b) Actual and the estimated fundamental Phasor. (c) Actual and the estimated 3rd harmonic Phasor. (d) Actual and the estimated 5th harmonic Phasor. Actual ---, proposed —.

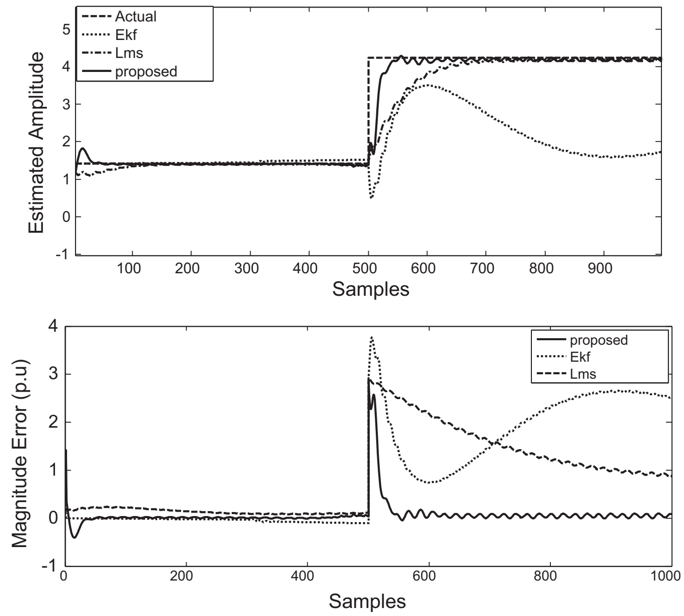

(a)

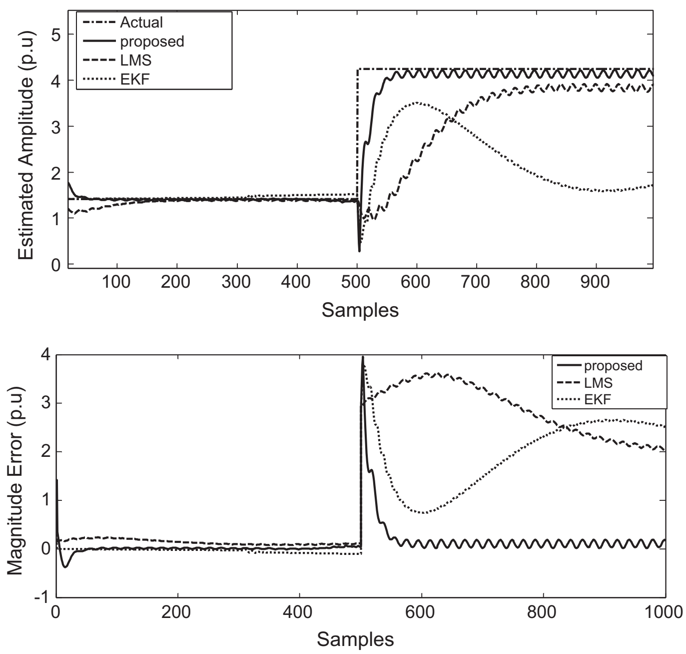

(b)

Fig. 8. (a) Estimated magnitude and magnitude error of different algorithms with frequency deviation (df = 1 Hz). (b) Estimated magnitude and magnitude error of different algorithms with frequency deviation (df = 2 Hz).

even in complicated situations. Fig. 8(b) plots the magnitude and phaseangle error in case when the frequency deviation increases from 1 Hz to 2 Hz. EKF [12] fails to estimate the magnitude of the signal under this type of variation, though LMS [44] shows some improvement in tracking however consumes more than two cycles to converge to its true value.

4.2.7. Case VIII: random frequency changes

To test the robustness of the proposed ADALINE filter two cases of random frequency change are initiated by the following expressions:

$$\begin{aligned} &case\ a.\ f(t) = f_0 + 2 \cdot (0.5 - rand(0,1)) \\ &case\ b.\ f(t) = f_0 + 2 \cdot (2 - rand(0,1)), \end{aligned} \quad \text{and } f_0 = 49.0\text{ Hz} \tag{81}$$

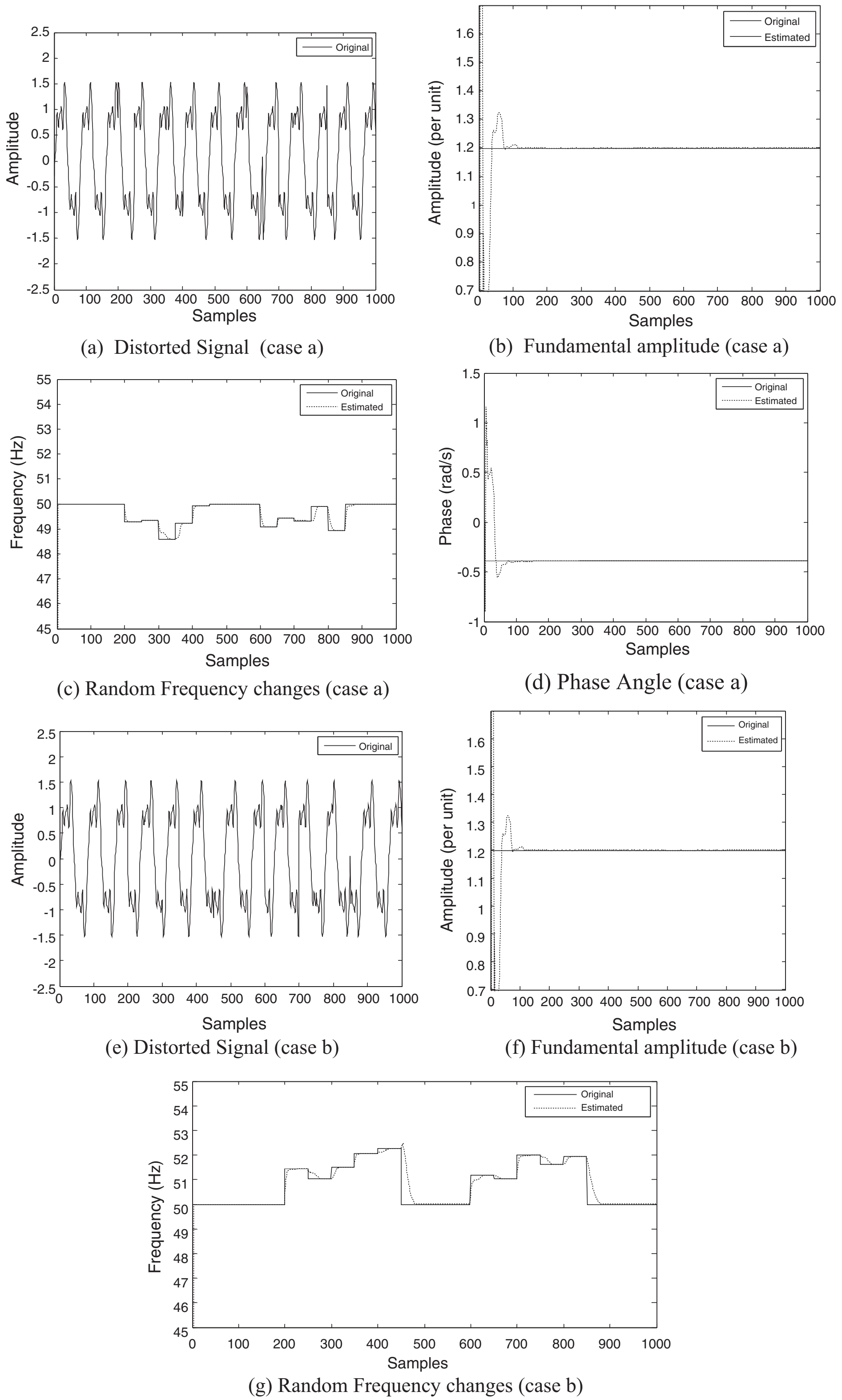

Fig. 9. Random frequency change (*case a*. $f(t) = f_0 + 2 \cdot (0.5 - rand(0,1))$ *case b*. $f(t) = f_0 + 2 \cdot (2 - rand(0,1)))$ where $f_0 = 49$.

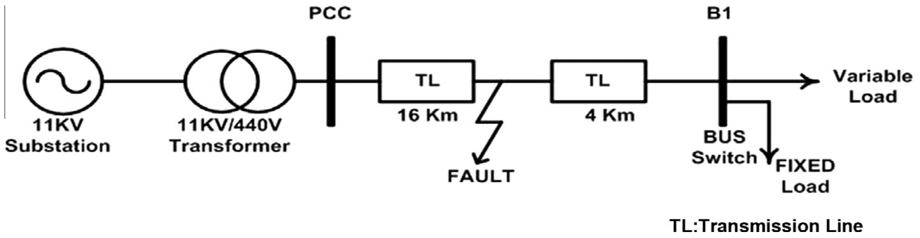

Fig. 10. Power system under study.

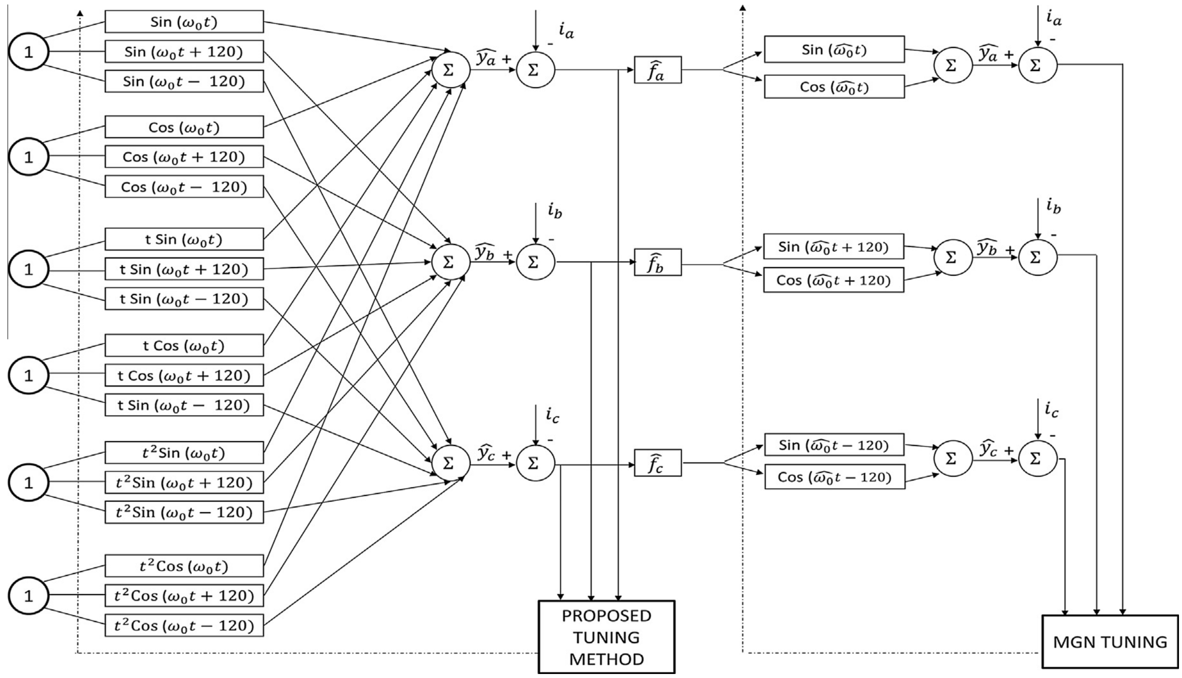

Fig. 11. Three-phase ADALINE schematic diagram.

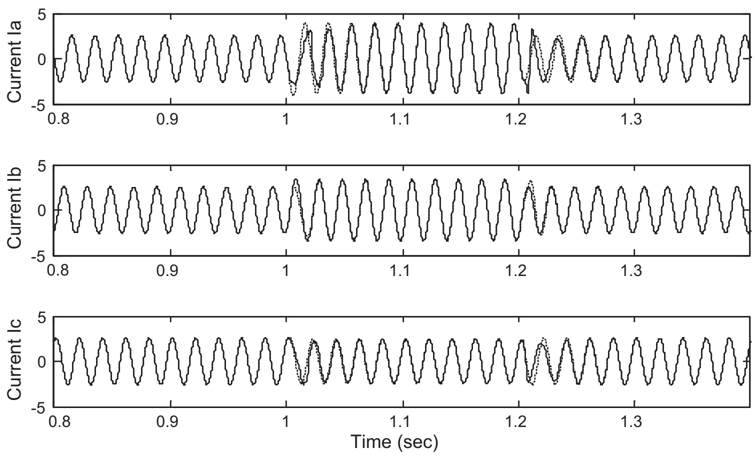

Fig. 12. Three-phase current signals during single-line-to-ground fault, Desired (solid line), Estimated (dotted).

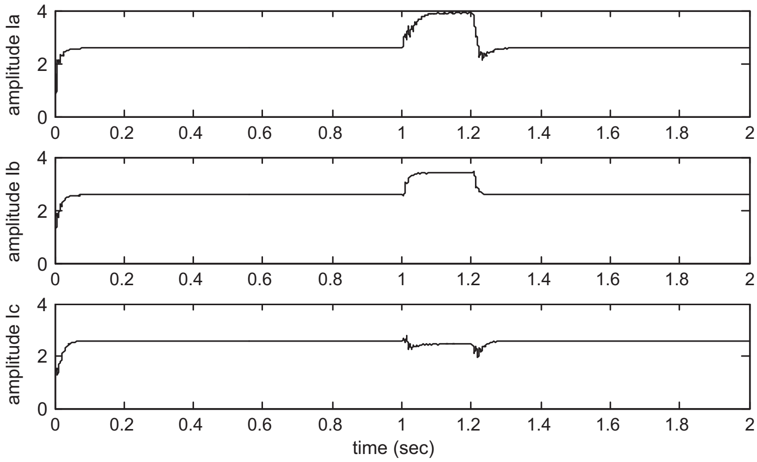

Fig. 13. Fault current peak amplitude of individual phase during single line-to-ground fault.

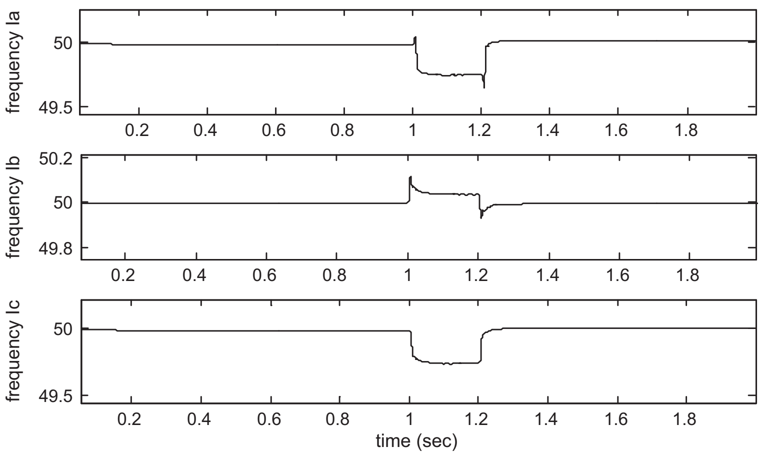

Fig. 14. Estimated frequency of the individual phases during single line-to-ground fault.

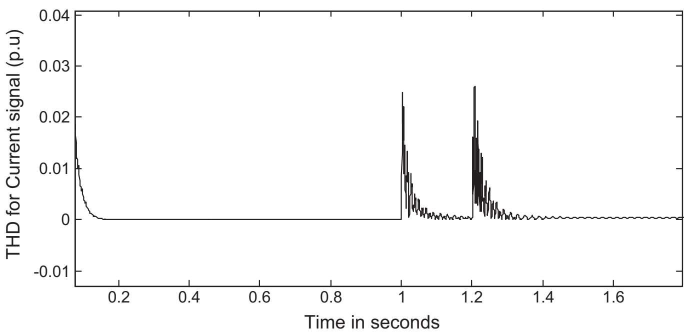

Fig. 15. Total harmonic distortion (THD) during fault.

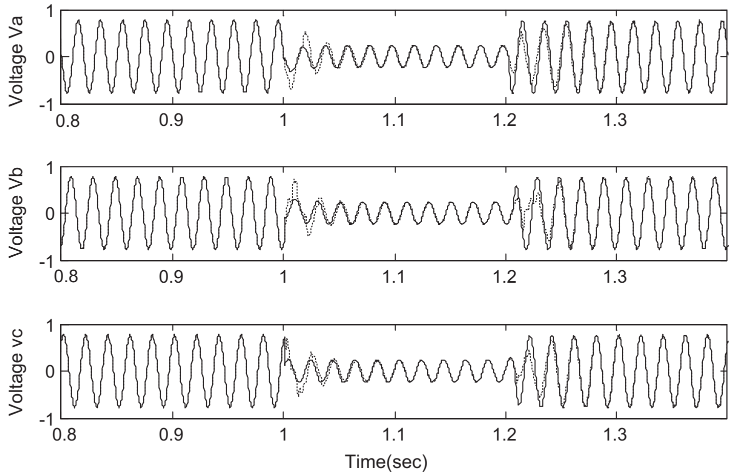

Fig. 16. Phase voltage waveforms during tripple line-to-ground fault, Desired (solid line), Estimated (dotted).

It is well known that small changes in fundamental frequency are difficult to track and it is also difficult to ascertain their impact on the power network performance. The signal considered for the test is given by

$$\begin{aligned} y(t) &= 1.2\sin\left(\omega t - \frac{\pi}{8}\right) + 0.4\sin\left(3\omega t - \frac{\pi}{6}\right) \\ &\quad + 0.2\sin(5\omega t) + 0.15\sin\left(7\omega t - \frac{2\pi}{3}\right) \\ &\quad + 0.1\sin\left(11\omega t - \frac{\pi}{10}\right) + \upsilon(t) \end{aligned} \tag{82}$$

where $\upsilon(t)$ is a white Gaussian noise of zero mean and SNR = 30 dB, and the angular frequency of the signal $\omega = 2\pi f(t)$. The random frequency changes are initiated from 200 sample points till 850 sample points after the normal frequency of 50 Hz is established. Fig. 9 exhibits the distorted signal, fundamental amplitude and phase angle, and the actual and tracked frequencies. From the figure it is quite obvious that the estimated parameters are almost equal to the actual ones and convergence time is extremely small in both the extreme cases of random frequency change which shows the robustness and sensitiveness of the proposed FVSS algorithm toward random and very small frequency variations which are common in power signal applications.

4.3. Using fault signal generated in MATLAB/Simulink

4.3.1. Case IX: transient test

To evaluate the performance of the proposed algorithm on a typical transmission system under transient condition, voltage and current signals are generated using MATLAB/Simulink software.

Fig. 10 shows the schematic diagram of the power system under study. A 11 kV substation is connected to a 440 V distribution network which has been modeled in Simulink to generate the waveform for testing. The algorithm can easily be modified to Multiple Output ADALINE shown in Fig. 11 for the analysis of three-phase voltage and current signals. A single line-to-ground fault is initiated at time $t = 1$ s and is cleared at $t = 1.2$ s. The three-phase voltage and current samples near the P.C.C (point of common coupling) are used as input to the algorithm for the estimation of various signal parameters.

Fig. 12 shows three phase current and the estimated signal, and Figs. 13 and 14 show the estimated amplitude and frequency of all the three-phase fault current signals. The total harmonic distortion (THD), is considered for evaluating the performance of the proposed algorithm. The equivalent total harmonic distortion factor for voltages is computed as [48]

$$V_{ub,THD} = \frac{\sqrt{\sum_{m=2}^{M}\left(V_{abm,rms}^2 + V_{bcm,rms}^2 + V_{cam,rms}^2\right)}}{\sqrt{\left(V_{ab1,rms}^2 + V_{bc1,rms}^2 + V_{ca1,rms}^2\right)}} \tag{81}$$

where $V_{abm,rms}$, $V_{bcm,rms}$, and $V_{cam,rms}^2$ represents the root mean square (rms) line-to-line voltages, in an unbalanced 3-phase system. Similarly the equivalent total harmonic distortion factor for current is computed as

$$I_{ub,THD} = \frac{\sqrt{\sum_{m=2}^{M}\left(I_{am,rms}^2 + I_{bm,rms}^2 + I_{cm,rms}^2\right)}}{\sqrt{\left(I_{a1,rms}^2 + I_{b1,rms}^2 + I_{c1,rms}^2\right)}} \tag{82}$$

where $I_{am,rms}$, $I_{bm,rms}$ and $I_{cm,rms}$ represent the phase-a, phase-b and phase-c RMS (root mean squares) current values.

From Fig. 15, it can be observed that, the total harmonic distortion for current signal remains within 2.5% using the proposed algorithm. In a similar way, the three-phase voltage signal with triple line-to-ground fault is taken as input to the proposed algorithm. Fig. 16 shows three-phase voltage signal and its estimated value, and Figs. 17–19 depict the estimated amplitude and frequency of the fault voltage signals, and the THD. It is clear from these figures that the proposed FVSS ADALINE filter is highly sensitive to sudden changes in frequency and amplitude during fault conditions and hence can be used as an efficient signal

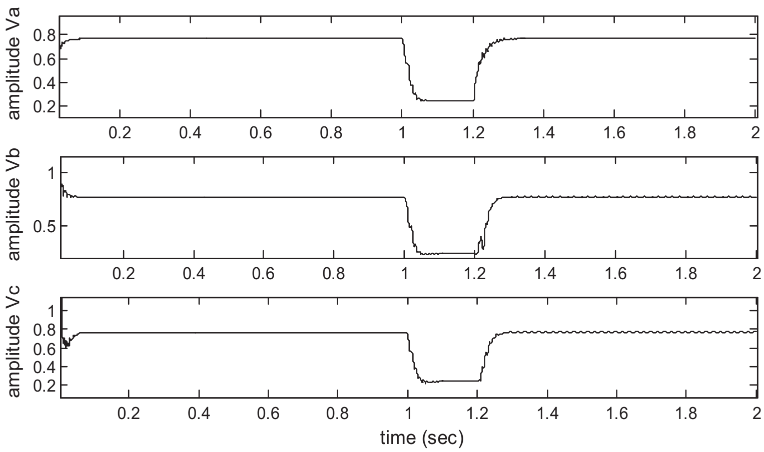

Fig. 17. Estimated peak voltage amplitudes of individual phases during triple line-to-ground fault.

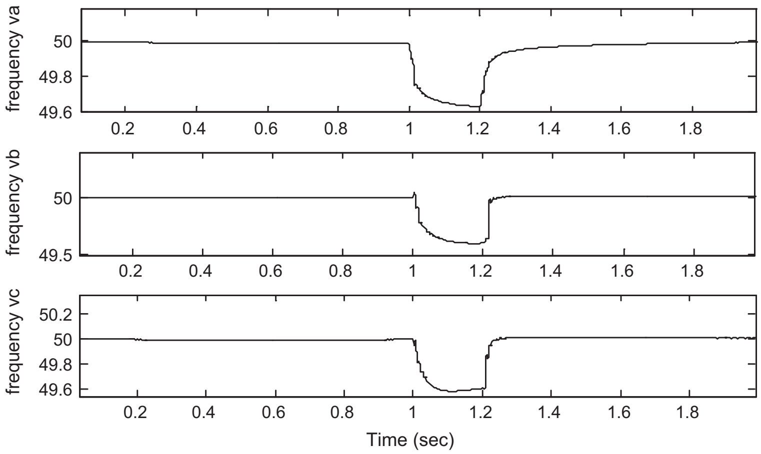

Fig. 18. Estimated peak frequencies of individual phases during triple line-to-ground fault.

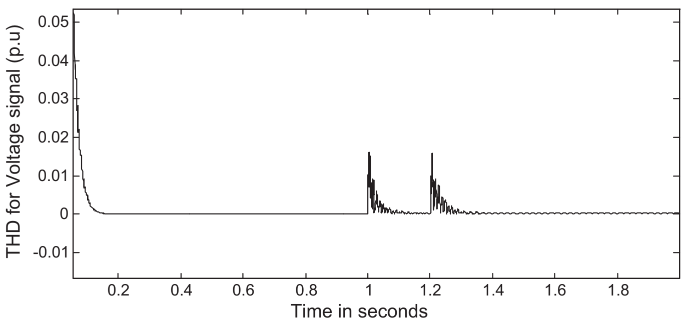

Fig. 19. Estimation of THD (voltage) during triple line-to-ground fault.

estimator. From Figs. 15 and 19 it can be seen that the THD is about 2.5% for current and 1.8% for voltage signals using the proposed method that is much below the 5.0% limit as provided by the IEEE Standard and thus meets the %THD requirements set by IEEE519 standard [49].

5. Conclusion

In this paper a new robust Fuzzy adaptive filter has been proposed for the accurate measurement of frequency, amplitude, and phase angle of voltage or current signals in a power network. The proposed method is tested under different noise condition under power swing, transient, step change, modulated change and short-circuit conditions and compared with some of the widely used algorithms using MATLAB/Simulink software. The new filter is based on estimating the frequency using the Taylor series expansion of the dynamic signal and the parameters are computed using a robust Fuzzy adaptive learning paradigm. The phasor of the dynamic signal are estimated using the modified Gauss–Newton algorithm for reduced computational overhead. The performance analysis clearly reveals that the proposed method eliminates sensitivity to noise and shows global convergence. A number of case studies is presented to support the efficacy of the proposed method that includes static signals, step changes, amplitude modulations and faults, etc. Mean of RMSE and THD are presented for obtaining a meaningful comparison with the existing methods. The new FVSS ADALINE filter exhibits accurate frequency, phasor estimation results under dynamic conditions and achieves good noise and harmonic rejection capabilities even under critical situations when the frequency of the utility voltage fluctuates from its nominal value. Also as shown the sampling frequency requirement of the proposed algorithm is within an acceptable range. Moreover the proposed approach consumes considerably less computations and uses a simple ADALINE structure which not only reduces the processing time but also system complexity that makes the proposed approach efficient to be implementable on an hardware platform. These advantages of the proposed approach are suitable to be used in smart integration modules which can be used in DG systems, control and monitoring of power quality issues, etc. In essence, the new approach can meet the critical demand of real-time applications like wide area monitoring, and protection of power system networks in a smart grid environment.

References

[1] H.J. Math, I.Y.H. Gu, Signal Processing of Power Quality Disturbances, Wiley, New York, 2006.

[2] R.C. Dugan, T.E. McDermott, Operating conflicts for distributed generation on distribution systems, in: Proc. Rural Electric Power Conf., 2001, pp. A3/1–A3/6.

[3] A. Bonner et al., Modeling and simulation of the propagation of harmonics in electric power networks, IEEE Trans. Power Delivery 11 (1) (1996) 452–465.

[4] C.T. Nguyen, K.A. Srinivasan, A new technique for rapid tracking of frequency deviations based on level crossings, IEEE Trans. Power Ap. Syst. 103 (8) (1984) 2230–2236.

[5] S.I. Jeng, J.H. Choi, J.W. Kim, D. Choi, An adaptive relaying for the protection of a wind farm interconnected with distribution network, in: IEEE PES Transmission and distribution Conf, vol. 1, 2003, pp. 296–302.

[6] Ch.Sh. Yu, A discrete Fourier transform based adaptive mimic phasor estimator for distance relaying application, IEEE Trans. Power Delivery 21 (4) (2006) 1836–1846.

[7] A.A. Girgis, F. Ham, A qualitative study of pitfalls in FFT, IEEE Trans. Aerospace Electron. Syst. AES 16 (1980) 434–439.

[8] G.W. Chang, C.I. Chen, Y.J. Liu, M.C. Wu, Measuring power system harmonics and interharmonics by an improved fast Fourier transform-based algorithm, Proc. IET Gener. Transm. Distrib. 2 (2) (2008) 193–201.

[9] He Wen, Siyu Guo, Zhaosheng Teng, Fuhai Li, Yuxiang Yang, Frequency estimation of distorted and noisy signals in power systems by FFT-based approach, IEEE Trans. Power Syst. 29 (2) (2014) 765–774.

[10] Dong-Guy Lee, Sang-Hee Kang, Soon-Ryul Nam, Modified dynamic phasor estimation algorithm for the transient signals of distributed generators, IEEE Trans. Smart Grid 4 (1) (2013) 419–424.

[11] E.A. Feilat, Detection of voltage envelope using Prony analysis-Hilbert transform method, IEEE Trans. Power Delivery 21 (4) (2006) 2091–2093.

[12] C.I. Chen, G.W. Chang, R.C. Hong, H.M. Lee, Extended real model of Kalman filter for time varying harmonics estimation, IEEE Trans. Power Delivery 25 (1) (2010) 17–26.

[13] Z.G. Zhang, S.C. Chan, K.M. Tsui, A recursive frequency estimation using linear prediction and a Kalman filter based iterative algorithm, IEEE Trans. Circ. Syst. II, Exp. Briefs 55 (6) (2008) 576–580.

[14] M.D. Kusljevic, J.J. Tomic, L.D. Jovanovic, Frequency estimation of three phase power system using weighted least square algorithm and adaptive FIR filtering, IEEE Trans. Instrum. Meas. 59 (2) (2010).

[15] C. Tao, D. Shanxu, R. Ting, L. Fangrui, A robust parametric method for power harmonic estimation based on M-estimators, Measurement 43 (1) (2010) 67–77.

[16] G.W. Chang, C.I. Chen, An accurate time domain procedure for harmonics and interharmonics detection, IEEE Trans. Power Delivery 25 (3) (2010) 1787–1795.

[17] S.K. Jain, S.N. Singh, Exact model order ESPRIT technique for harmonics and interharmonics estimation, IEEE Trans. Instrum. Meas. 61 (7) (2010) 1915–1923.

[18] J. Ren, M. Kezunovic, A hybrid method for power system frequency estimation, IEEE Trans. Power Delivery 27 (3) (2012) 1252–1259.

[19] C. Dotta, J. Chow, Second harmonic filtering in phasor measurement estimation, IEEE Trans. Power Delivery 28 (2) (2013) 1240–1241.

[20] P.J. Moor, J.H. Allemeling, A.T. Johns, Frequency relaying based on instantaneous frequency measurement, IEEE Trans. Power Delivery 11 (4) (1996) 1737–1742.

[21] Y. Guo, M. kezunovic, Simplified algorithms for removal of the effect of exponentially decaying DC-offset on the Fourier algorithms, IEEE Trans. Power Delivery 18 (3) (2003) 711–717.

[22] V.L. Pham, K.P. Wong, Antidistortion method for wavelet transform filter banks and nonstationary power system waveform harmonic analysis, Proc. Inst. Electr. Eng., Gen. Transm. Distrib. 148 (2) (2001) 117–122.

[23] J. Ren, M. Kezunovic, Real-time power system frequency and phasors estimation using recursive wavelet transform, IEEE Trans. Power Delivery 26 (3) (2011).

[24] M. Niedzwickei, P. Kaczmarek, Tracking analysis of a generalized Notch filters, IEEE Trans. Signal Process. 54 (1) (2006) 304–314.

[25] Sanf-Wook Sohn, Young-Bin Lim, Jae-Jun Yun, Hun Choi, Hyeon-Deok Bae, A filter bank and a self- tuning adaptive filter for the harmonic and inter harmonic estimation in power signals, IEEE Trans. Instrum. Meas. 61 (1) (2012) 64–73.

[26] Innocent Kamwa, S.R. Samantaray, Geza Joos, Fellow, wide frequency range adaptive phasor and frequency PMU algorithms, IEEE Trans. Smart Grid 5 (2) (2014) 569–579.

[27] H. Mori, An artificial neural network based method for power system voltage harmonics, IEEE Trans. Power Delivery-7 1 (1992) 402–409.

[28] P.K. Dash, D.P. Swain, A. Routry, A.C. Liew, Harmonic estimation in a power system using adaptive perceptrons, IEE Proc.-Gener. Transm. Distrib. 143 (6) (1996) 565–574.

[29] D.O. Abdeslam, P. Wira, J. Merckle, D. Flieller, Y.-A. Chapuis, A unified artificial neural network architecture for active power filters, IEEE Trans. Ind. Electron. 54 (1) (2007) 61–76.

[30] B.K. Bose, Neural network applications in power electronics and motor drives—an introduction and perspective, IEEE Trans. Ind. Electron. 54 (1) (2007) 14–33.

[31] I.C. Cheng, Virtual multifunction power quality analyzer based on adaptive linear neural network, IEEE Trans. Ind. Electron. 59 (8) (2012) 3321–3329.

[32] Gary W. Chang, Cheng-I. Chen, Quan-Wei Liang, A two stage ADALINE for harmonic and inter harmonic measurement, IEEE Trans. Ind. Electron. 56 (6) (2009) 2220–2228.

[33] S. Tong, Y. Li, G. Feng, T. Li, Observer-based adaptive fuzzy backstepping dynamic surface control for a class of MIMO nonlinear systems, IEEE Trans. Syst. Man Cybern. 41 (4) (2011).

[34] S. Tong, Y. Li, P. Shi, Observer-based adaptive fuzzy backstepping output feedback control of uncertain MIMO pure-feedback nonlinear systems, IEEE Trans. Fuzzy Syst. 20 (4) (2012) 771–785.

[35] S. Tong, S. Sui, Y. Li, Fuzzy adaptive output feedback control of MIMO nonlinear systems with partial tracking errors constrained, IEEE Trans. Fuzzy Syst. 23 (4) (2015).

[36] W.S. Chen, L.C. Jiao, R.H. Li, J. Li, Adaptive backstepping fuzzy control for nonlinearly parameterized systems with periodic disturbances, IEEE Trans. Fuzzy Syst. 18 (4) (2010) 674–685.

[37] T.P. Zhang, H. Wen, Q. Zhu, Adaptive fuzzy control of nonlinear systems in pure feedback form based on input-to-state stability, IEEE Trans. Fuzzy Syst. 18 (1) (2010) 80–93.
[38] S. Mitchell, K. Cohen, Fuzzy logic decision making for autonomous robotic applications, in: IEEE 6th International Conference Awareness Science and Technology (iCAST), 29–31 October 2014, pp. 1–6.
[39] C. Laopromsukon, K. Hongesombut, J. Rungrangpitayagon, Wide-area power system control using Fuzzy logic based static synchronous series compensator, in: Electrical Engineering Congress (iEECON), 2014, 19–21 March 2014.
[40] R. Belaidi, A. Haddouche, H. Guendouz, Fuzzy logic controller based three-phase shunt active power filter for compensating harmonics and reactive power under unbalanced mains voltages, Energy Procedia 18 (2012) 560–570.
[41] P.K. Dash, Shazia Hasan, A fast recursive algorithm for the estimation of frequency, amplitude, and phase of noisy sinusoid, IEEE Trans. Ind. Electron. 58 (10) (2011).
[42] S. Hasan, P.K. Dash, S. Nanda, A signal processing adaptive algorithm for nonstationary power signal parameter estimation, Int. J. Adapt. Control Signal Process. 27 (3) (2013) 166–181.
[43] J. Ren, M. Kezunovic, An improved Fourier method for power system frequency estimation, in: North American Power Symposium (NAPS), 4–6 August, Boston, MA, 2011, pp. 1–6.
[44] Sun Yong-mei, Duan Xiao-xia, Zhao Wei, Kan Yuan-yuan, Novel variable step-size adaptive LMS time delay estimation algorithm with nonlinear preprocess, in: 4th International Congress on Image and Signal Processing, 2011, pp. 2767–2770.
[45] Ting-Ting Li, Min Shi, Qing-Ming Yi, An improved variable step-size LMS algorithm, in: Wireless Communications, Networking and Mobile Computing (WiCOM), 7th International Conference, 23–25 September, Wuhan, 2011, pp. 1–4.
[46] H.C. So, A comparative study of three recursive least squares algorithms for single-tone frequency tracking, Signal Process. 83 (9) (2003) 2059–2062.
[47] Jun Zheng, Kenneth W.K. Lui, W.-K. Ma, H.C. So, Two simplified recursive Gauss–Newton algorithms for direct amplitude and phase tracking of a real sinusoid, IEEE Signal Process. Lett. 14 (12) (2007).
[48] M. Padhi, P.K. Dash, K.R. Krishnand, P.K. Rout, A fast Gauss-Newton algorithm for islanding detection in distributed generation amplitude and phase tracking of a real sinusoid, IEEE Trans. Smart Grid 3 (3) (2012).
[49] IEEE Recommended Practices and Requirements for Harmonics Control in Electric Power Systems, IEEE Std. 519, 1992.